

MIT Open Access Articles

Amide I'-II' 2D IR spectroscopy provides enhanced protein secondary structural sensitivity

The MIT Faculty has made this article openly available. **Please share** how this access benefits you. Your story matters.

Citation: DeFlores, Lauren P. et al. "Amide I#-II# 2D IR Spectroscopy Provides Enhanced Protein Secondary Structural Sensitivity." *Journal of the American Chemical Society* 131.9 (2009): 3385-3391.

As Published: <http://dx.doi.org/10.1021/ja8094922>

Publisher: American Chemical Society

Persistent URL: <http://hdl.handle.net/1721.1/69554>

Version: Author's final manuscript: final author's manuscript post peer review, without publisher's formatting or copy editing

Terms of Use: Article is made available in accordance with the publisher's policy and may be subject to US copyright law. Please refer to the publisher's site for terms of use.



Amide I'-II' 2D IR spectroscopy provides enhanced protein secondary structural sensitivity

Lauren P. DeFlores, Ziad Ganim, Rebecca A. Nicodemus, and Andrei Tokmakoff*

Department of Chemistry, Massachusetts Institute of Technology, Cambridge, MA 02139, USA

**Corresponding author: tokmakof@mit.edu*

Abstract

We demonstrate how multi-mode 2D IR spectroscopy of the protein amide I' and II' vibrations can be used to distinguish protein secondary structure. Polarization-dependent amide I'-II' 2D IR experiments on poly-L-lysine in the β -sheet, α -helix, and random coil conformations show that a combination of amide I' and II' diagonal and cross peaks can effectively distinguish between secondary structural content where amide I' infrared spectroscopy alone cannot. The enhanced sensitivity arises from frequency and amplitude correlations between amide II' and amide I' spectra that reflect the symmetry of secondary structures. 2D IR surfaces are used to parameterize an excitonic model for the amide I'-II' manifold suitable to predict protein amide I'-II' spectra. This model reveals that the dominant vibrational interaction contributing to this sensitivity is a combination of negative amide II'-II' through-bond coupling and amide I'-II' coupling within the peptide unit. The empirically determined amide II'-II' couplings do not significantly vary with secondary structure: -8.5 cm^{-1} for the β sheet, -8.7 cm^{-1} for the α helix, and -5 cm^{-1} for the coil.

Introduction

Amide vibrational spectroscopy¹ is an important tool for characterizing protein structure and dynamics with picosecond time-resolution.² The amide vibrations are intrinsic to the protein backbone and have secondary structure sensitivity. Unlike traditional protein infrared spectroscopy, which has the practical limitation of congested lineshapes, emerging methods in two-dimensional infrared (2D IR) spectroscopy are providing substantially more detailed methods for analyzing the structural and dynamical information content of these vibrations.^{1,3-11} 2D IR spreads infrared transitions over two frequency axes and reveals cross peaks that quantify vibrational couplings and other correlations between vibrations. The combination of enhanced spectroscopic sensitivity and a new generation of structure-based amide spectroscopic models^{3,12-15} is leading to a toolset that can be used for the quantitative study of time-dependent protein conformation.¹⁶ While protein 2D IR spectroscopy has primarily targeted the structure sensitive amide I band, the use of multi-mode 2D IR spectroscopy that investigates cross-correlations between different amide vibrations opens entirely new possibilities for enhancing structural information in protein vibrational spectra. In this paper, we report such an advance in which amide I'-II' 2D IR spectroscopy is used to give enhanced protein secondary structural sensitivity.

The most studied protein vibration, amide I, is composed predominately of peptide carbonyl stretch and displays secondary structure sensitivity. Empirical frequency-structure correlations find that β -sheets have a strong absorption band at 1610–1640 cm^{-1} and a weaker band at 1680-1690 cm^{-1} . The α -helix and random coil structure are located at 1640–1650 cm^{-1} and 1650–1660 cm^{-1} , respectively.^{17,18} The origin of these

band shifts is a strong coupling between individual amide I units which gives rise to delocalized or excitonic vibrational states that report on the symmetry and size of secondary structure^{2,19}. While anti-parallel β sheets and aggregates give rise to distinct diagnostic amide I bands⁸, other secondary structures are poorly resolved in an amide I line shape with multiple contributions. The α -helical structure is predicted to have three IR active amide I modes, but their splittings are on the order of a few cm^{-1} and the features are not resolvable.

The amide II vibration, due to its composition of NH bend and CN stretch, is predominately known for its sensitivity to the protonation state of the peptide unit.²⁰ Its 100 cm^{-1} frequency downshift between protonated (amide II) and deuterated (amide II') forms can be used with kinetic H/D exchange experiments to probe water exposure of protein structure.²¹ Despite early predictions of Miyazawa and Blout²² that amide II would exhibit sensitivity similar to amide I, the amide II band is relatively unstructured and varies little with secondary structure. In the case of amide II', the congested nature of the linear IR spectrum, as well as its overlap with the HOD bend absorption, makes its use as a structural diagnostic impractical.

This work uses 2D IR to resolve details of the 2D amide II' lineshape and investigate the amide I'-II' cross-peaks in a model system that adopts different secondary structures, poly-L-lysine (PLL). 2D IR cross peaks are used to characterize secondary structure specific spectral features. It is found that the amide II' 2D line shape gives rise to distinctive signatures for α helices and random coil regions, which, when combined with the β sheet sensitivity of the amide I region, allow for separation of all the common secondary structural motifs. Polarization dependent experiments are used to quantify

vibrational couplings and transition dipole orientations between amide II' oscillators and between amide I' and II', and also describe the symmetry of the modes involved. 2D IR spectra are interpreted with an excitonic model for the amide I'-II' manifold suitable to predict protein amide I'-II' FTIR and 2D IR spectra. The mechanism for vibrational coupling that leads to these structure-sensitive spectra is revealed to be a combination of through-bond coupling between amide II' local modes in addition to a strong amide I'-II' coupling at a given peptide unit. This supports recent theoretical observations^{13,23} and provides clear evidence against the widely made assumption that the amide vibrations are orthogonal and therefore energetically isolated.

Methods and Materials

Materials. All samples are purchased from Sigma-Aldrich (St. Louis, MO). Before use, samples were fully deuterated by hydrogen/deuterium exchange in D₂O at 45°C for 1 hour, followed by lyophilization. Samples were held in a temperature-controlled cell with 1-mm thick calcium fluoride windows and a 50 μm path length. Concentrations of the polypeptide forms are selected such that the infrared absorbance of the amide I' band is <0.5; approximately 20 mg/mL. Poly-L-lysine samples are prepared under different conditions in order to generate the desired secondary structure motif.²⁴ The random coil species is prepared by dissolving the protein in neat D₂O at 20 °C and pH = 4.0.²⁵ The α-helical conformation is prepared by dissolving PLL into neat D₂O and raising the pH to 12 using 1M NaOD solution. The β-sheet form of PLL is prepared by subsequently raising the temperature of the α-helical solution to 46°C over 30 minutes. Spectra of the helical and sheet moieties were taken consecutively on identical samples. Protein samples were prepared in a 50 mM phosphate buffer.

2D IR Spectroscopy. 2D IR experiments are performed with bandwidth sufficient to cover the fundamental and overtone bands of amide I' and amide II' using a 2D FT spectrometer that is described in detail elsewhere.²⁶ The mid-infrared laser pulse was centered at 1550 cm^{-1} with a FWHM bandwidth of approximately 350 cm^{-1} and compressed to sub-80 fs in duration. 2D IR spectra are acquired in a two-beam geometry using a collinear pulse pair to pump and third pulse to serve as the probe and local oscillator. ZZYY spectra were collected by rotation of the probe polarization through a 90° turn periscope. The excitation dimension is obtained by step scanning the τ_1 time axis to 1.8 ps in steps of 2 fs giving a resolution of $\sim 1 \text{ cm}^{-1}$. The transmitted probe is dispersed in a monochromator using a 75-groove/mm grating and collected using a 64 pixel MCT array detector. The 1.9 cm^{-1} resolution in the ω_3 detection axis results in a 120 cm^{-1} single-scan detection bandwidth. 2D spectra are assembled from spectrograms centered at 1450 cm^{-1} and 1650 cm^{-1} . Fourier transformation of the signal as a function of the timing between pump pulses (τ_1) resolves the 2D spectrum along the ω_1 axis.

Structure Based Modeling. Modeling of amide I'-II' spectra drew on idealized structures for an anti-parallel β sheet, α helix, and random coil. Molden²⁷ was used to generate an idealized anti-parallel β sheet consisting of six strands with seven peptide units per strand by repeating $\phi=-139^\circ$ and $\psi=135^\circ$. The strands have co-planar C_α spaced 3.04 Å apart. A 20 residue α helix was generated by repeating $\phi=-57^\circ$ and $\psi=-47^\circ$. Calculations for the random coil involved an average over 5000 snapshots of a GROMACS^{28,29} molecular dynamics simulation of an 18-oscillator peptide with rigid bond lengths³⁰ and angles in vacuum, coupled to a 1000 °C bath.³⁰

Analogous to previous work¹², amide I'-II' spectra are calculated by diagonalizing a local mode Hamiltonian developed in the basis of the amide I' and II' vibrations for the individual peptide units. The elements of this local amide Hamiltonian are assigned on the basis of the position of the peptide units within the structure. The amide II' Hamiltonian parameters are experimentally constrained and appear in the *Local Mode Modeling* section. The amide I' vibrations are characterized by anharmonically coupled oscillators with empirically chosen, degenerate site energies of 1675 cm⁻¹ and anharmonicity of 16 cm⁻¹.³ Non-bonded amide I'-I' interactions were determined through transition dipole coupling.³¹ The orientation of the amide I' transition dipole was set 20° off the C=O bond, with the dipole center located 0.868 Å along the carbonyl axis,²⁰ and a normalized unit dipole strength of 1.0. Spectral calculations involved a sum over transition pathways between eigenstates weighted by polarization factors including two-quantum states through a weak anharmonicity and harmonic scaling of the transition moments.⁸ Calculation averaged over a static disordered system using a homogeneous linewidth (FWHM) of 14 cm⁻¹.

Results and Discussion

Linear Spectroscopy of Amide I' and II'

The FTIR spectra of the three forms of poly-L-lysine are shown in Fig. 1. Unlike the spectra of the single peptide unit in N-methylacetamide,³² the amide I' and amide II' bands are structured. In random coil form, poly-L-lysine shows a small shoulder on the blue side of the amide I' band maximum (1645 cm⁻¹), and is broad and suggestive of overlapping resonances in the amide II' band. In the α -helical form, the amide I' band is

red-shifted and asymmetric. This lineshape is commonly interpreted as the overlapping contributions from the intense *A* band near 1630 cm^{-1} (ν_A) and the weaker blue-shifted *E* bands (ν_E). The amide II' band shows a distinct two peak structure. As the temperature of the α -helical form is increased, PLL undergoes a structural transition into a β -sheet aggregate. In β -sheet form, the amide I' band splits into the signature high and low intensity β -sheet modes. The 1610 cm^{-1} and 1690 cm^{-1} modes are termed ν_{\perp} and ν_{\parallel} , respectively, to refer to whether the amide I oscillators of the mode vibrate in-phase perpendicular or parallel to the strands of the sheet. For the β sheet, amide II' does not exhibit such a drastic change, but rather loses structure.

2D IR Spectroscopy of Amide I' and II'

The 2D IR spectra of PLL in the various secondary structure conditions are shown in Fig. 2 for parallel (ZZZZ) and perpendicular (ZZYY) polarized probing. Spectral regions of interest include the lineshapes of the amide I' ($\omega_1, \omega_3 = 1600\text{-}1700\text{ cm}^{-1}$) and II' ($\omega_1, \omega_3 = 1400\text{-}1500\text{ cm}^{-1}$) diagonal regions, and the amide I'-II' cross peaks. As expected from its low cross-section, no signal contributions from the HOD bend were observed in the amide II' region. The secondary structural sensitivity revealed by describing the contours of the 2D lineshapes, which result from interference between positive (fundamental) and negative (overtone) transitions within the amide band. In addition, since the cross peak intensity scales quadratically with the dot product of the diagonal transition dipole moments, it encodes both the magnitude and the relative angle between the transition dipoles. Comparison of the cross peak amplitude as a function of polarization reveals the angle.³³ Qualitatively, the strong enhancement of a cross peak in

crossed polarization indicates a transition dipole projection angle close to orthogonal ($>70^\circ$), while a decrease indicates angles closer to parallel. The 2D IR spectroscopy of the diagonal amide I' line shape has been described previously.^{1,34}

The amide I' region of Fig. 2a shows the characteristic 8-peak structure for extended β -sheets, which arises from fundamental and overtone transitions of the ν_\perp and ν_\parallel vibrations and cross-peaks between them. The amide I'-I' cross peaks are enhanced in the perpendicular spectra in Fig. 2b, and a comparison of the cross peak amplitudes in parallel and perpendicular spectra³⁵ gives an angle between their transition dipoles of $\Theta_{I'\parallel-I'\perp}=67\pm7^\circ$, consistent with our previous measurement.¹ Similar to amide I', the diagonal amide II' region shows two peaks ($\omega_1, \omega_3=1440\text{ cm}^{-1}$ and 1490 cm^{-1}) and an enhancement of the cross peak between them in the perpendicular spectrum. Analysis of this cross peak amplitude variation is limited due to interference effects, but puts a constraint on their orientation $\Theta_{II'\parallel-II'\perp} > 35^\circ$.

The amide I' regions of the α -helix and random coil 2D spectra are similar, and it is difficult to distinguish between the two moieties using only the amide I' mode. The random coil lineshape is more diagonally elongated ($\omega_1 = \omega_3$) than the α helix. The amide I' α helix lineshape also shows slight off-diagonal broadening that is consistent with previous interpretations of two underlying A and E_1 symmetry modes³⁶⁻³⁸. However, examination of the diagonal amide II' region of the parallel spectra in Fig. 2c and 2e reveals distinct differences; the random coil line shape is again diagonally elongated while the α helix shows two peaks at 1470 cm^{-1} and 1440 cm^{-1} . Surprisingly, both the α helix and random coil show off-diagonal broadening in the perpendicular spectra. This arises from a plateau ($\omega_3=1480\text{ cm}^{-1}$) indicative of a cross-peak between two modes. The

presence of two peaks in the coil spectrum indicates that significant amide II' vibrational couplings persist in this state. A clearer indication of the amide II' structural sensitivity is seen in a projection of the perpendicular lineshape onto ω_3 , shown in Fig. 3a. Two distinct peaks are observed for the sheet and coil conformations, and the helix resonance is peaked between them. The multimode structure present in the random coil spectrum is an indication that the amide II' lineshape is reporting on local backbone configurational variation rather than the longer range structure of the entire chain.

Amide I'-II' Cross Peaks

Cross peaks between amide I' and amide II' allow the new spectral features of amide II' to be assigned by correlation to understood amide I' signatures. Both upward ($\omega_1 < \omega_3$) and downward ($\omega_1 > \omega_3$) cross peaks appear. The perpendicular β -sheet spectrum shows cross peaks between both pairs of the amide I' and II' modes. The most intense cross-peak to amide I' ν_{\perp} varies with polarization; inspection of the upward cross peaks along the slice $\omega_3 = 1611 \text{ cm}^{-1}$ shows that in perpendicular polarization the more intense cross peak is to the 1447 cm^{-1} amide II' band, while in the parallel polarization the cross peak to the 1470 cm^{-1} amide II' band is more intense. This intensity flipping is visible, albeit more subtle, in the cross-peaks of the amide I' ν_{\parallel} band to amide II' (along $\omega_3 = 1690 \text{ cm}^{-1}$). The alternating intensity of the cross peaks between amide I' and II' indicates that the low frequency ν_{\perp} amide I' (1611 cm^{-1}) and the high frequency amide II' (1470 cm^{-1}) modes have aligned transition dipoles which are nearly orthogonal to those of the high frequency ν_{\parallel} amide I' (1690 cm^{-1}) and low frequency amide II' (1447 cm^{-1}) modes. In the reference frame of the protein, if the transition dipole of the more intense

amide I' mode ν_{\perp} is aligned perpendicular to the β strands, then the transition dipole of the more intense amide II' mode (1447 cm^{-1}) is close to parallel with them. Therefore we assign the 1470 cm^{-1} band to the amide II' ν_{\perp} mode and the 1447 cm^{-1} band to the amide II' ν_{\parallel} mode of the β sheet.

The amide I'-II' upward cross peak in α -helical PLL is broad and shows an anti-diagonal elongation. (Fig. 2d). This implies that the frequency shift of the amide II' *A* and *E* modes are anti-correlated with the frequency shift in amide I'. The dramatic intensity increase of the downward cross peak from parallel to perpendicular spectra (Fig. 2c to 2d) implies a near perpendicular projection angle between the dominant amide I' and II' transition dipoles of the α helix. Since the *A* mode dominates the amide I' spectrum, the amide II' spectrum will be dominated by the helix mode with E_I symmetry. Marsh and coworkers³⁹ tabulate the angles of amide I and II relative to the helix axis to be $29\text{-}40^\circ$ and $73\text{-}77^\circ$, respectively. We can compare these results on amide II to our amide II' measurements drawing on the previous characterization of dipole projection angles for NMA- h_7 and NMA- d_7 .³² These show a very small angle between amide I and I' and a roughly 35° angle between amide II and II' transition moments. From this, one would predict that the transition dipole of amide II' lies between $108\text{-}112^\circ$ to the helix axis, giving a $72\text{-}79^\circ$ angle between amide I' and II', which is consistent with the results observed here. Our results indicate that transition dipole of the dominant amide II' band of α -helical PLL lies nearly perpendicular to the helix axis. From these observations, we assign the 1470 cm^{-1} and 1440 cm^{-1} vibrations to the amide II' *E* and *A* modes, respectively. In addition, the downward cross-peak of the helical PLL in both *ZZZZ* and

ZZYY 2D spectra show a weak negative transition. This is a distinguishing attribute relative to the random coil conformation.

For the coil spectra, the presence of an antidiagonal tilt to the perpendicularly polarized cross peak region, the presence of two peaks in the amide II' diagonal region, and a diagonally elongated amide I' diagonal peak together indicate that there are delocalized or excitonic amide I' and II' states in this species. Although the chain may be disordered, this should not be surprising, given the strength of amide I'-I' and amide II'-II' couplings between bonded peptide groups. While we expect a complex band structure to this feature, for preliminary assignment, we expect that the more intense red side of the amide II' band (1460 cm^{-1}) involves symmetric (+) motion between the CN stretches of bonded neighbors, whereas the weaker (1480 cm^{-1}) has antisymmetric (-) character. From the antidiagonal tilt of the amide I'-II' cross peak, we associate the red and blue sides of the amide I' band (1650 and 1670 cm^{-1}) with modes of + and - character, respectively.

A summary of the peak assignments to vibrations and the quantitative analysis of the projection angles between modes is presented in Table 1. These values of the projection angles and their constraints are determined using the ratio of peak amplitudes in parallel and perpendicular geometries assuming the rules for two coupled vibrations and that the ratio for the dominant diagonal peaks is 1/3. Interference effects reduce the ability to separate each of the possible angles, and typically lead to a lower bound on the projection angle. Of the PLL conformations, the β sheet spectra provide the highest number of constraints. We note that the β sheet projection angles cannot be easily reconciled with the constraint that they lay within a plane. This suggests that twisting of

the sheet and/or stacking of multiple sheets may be the origin of these angles. Additionally, we note that there is limited evidence that the sheet form of PLL is does indeed have antiparallel registry. It remains possible that the sheet for of PLL is an aggregate with the parallel in-register cross-beta structure seen in amyloid fibrils.

The greatest complement that amide II' adds to amide I' 2D IR spectroscopy is the ability to separate α -helix and random coil signatures. In addition to differences in the amide II' 2D lineshape, the random coil amide I'-II' upward and downward cross peaks are both more anti-diagonally elongated and the downward cross peak shows a strong negative transition. All together, amide I'-II' 2D IR spectroscopy allows clear separation of β sheets, α helices, and random coil structural motifs.

The enhanced secondary structure sensitivity of the amide I'-II' cross peak is more clearly seen as projections of the downward cross-peak lineshape onto the axis in Fig. 3b. These projections provide distinct spectral signatures for the three secondary structures. The sheet and coil both show a two-peak structure, but the more intense band is red shifted for the sheet and blue shifted for the coil. The helix is dominated by one resonance that lies between the others.

As an indication of how amide I'/II' 2D IR spectra would be used in the analysis of proteins, we have acquired spectra for four proteins that vary in the secondary structure content (Fig. 5). The presence of cross peaks in the amide I' ($\sim 1650\text{ cm}^{-1}$)/II' ($\sim 1450\text{ cm}^{-1}$) and amide I ($\sim 1650\text{ cm}^{-1}$)/II ($\sim 1550\text{ cm}^{-1}$) regions of Concanavalin A, a β -protein, and myoglobin, an α -protein, indicate partial hydrogen-deuterium exchange.²¹ Non-exchanging peptides within the Con A β -sheets are seen by the vertically displaced doublet for the amide I/II cross peak. The random coil content has exchanged and is seen

as intensity between this doublet of the amide I'/II' region. Myoglobin shows similar features to partially exchanged helical content. The intensity of the downward cross peak overtone shows a direct signature of exchanged random coil. Ubiquitin and RNaseA, mixed β -sheet and helical proteins, show full exchange under these conditions. Cross peaks show a super-position of all secondary structure motifs.

Local Mode Modeling of Amide I'-II' Spectra

To gain further insight into the origin of secondary structure sensitivity in amide I'-II' spectra and a detailed molecular assignment of the spectral features, we have constructed a structure-based model suitable for calculating amide I'-II' spectra of proteins. This modeling expands the local amide Hamiltonian (LAH) approach that has been successful in predicting amide I' 2D IR spectra and providing frequency-structure correlations.^{3,12} The amide I'-II' manifold of vibrations is described as a linear combination of unit amide I' and II' oscillators on each peptide group. The LAH is constructed in this basis and the elements are assigned using a structure. The diagonal elements (site energy) correspond to the intrinsic vibrational frequency of that isolated oscillator, and off-diagonal terms (coupling between oscillators) depend on their separation and orientation. Diagonalizing the LAH allows us to calculate FTIR and 2D IR spectra for a given structure.

The amide I' block of the local amide Hamiltonian (LAH) is constructed as previously described³¹ (details appear above) and amide II' is added with the minimum number of extra variables. This reflects two assumptions: (1) For simplicity we assume the amide II' oscillators couple with each other only as a result of through-bond interactions with their neighbors in the chain. This is expected given the small transition

dipole moment and unfavorable position for through space amide II' couplings. (2) Similarly, we assume that amide I' and II' vibrations only couple within the same peptide unit. This assumption is reasonable since the strength of the on-site coupling in NMA is far greater than all other interactions involving amide I and II^{13,32}.

Parameters for the LAH are obtained from prior amide I'-II' 2D IR experiments on NMA-d₇ in D₂O.³² We set the amide II' site energy to $\omega_{II'} = 1450 \text{ cm}^{-1}$, the amide II' vibrational anharmonicity to $\Delta_{II'} = 10 \text{ cm}^{-1}$, the amide I'-II' on-site coupling to $V_{I'-II'} = 39 \text{ cm}^{-1}$, and the transition dipole ratio $\mu_{AmII'}/\mu_{AmI'} = 0.58$. To match the random coil lineshape, the amide I' and amide II' site energies are sampled from a normal distribution with standard deviation of 10 cm^{-1} about the assigned $\omega_{I'}$ and $\omega_{II'}$ values. Amide II'-II' coupling between nearest neighbor sites were set with empirically determined values to $V_{II'-II'} = -8.5 \text{ cm}^{-1}$ for the β sheet, -8.7 cm^{-1} for the α helix, and sampled from a normal distribution ($\langle V_{II'-II'} \rangle = -5 \text{ cm}^{-1}$ and $\sigma = 3 \text{ cm}^{-1}$) for the random coil. These idealized structures are our best approximations to the unknown atomic structures of poly-L-lysine, which may contain nonregular, fibrillar structures.⁴⁰ The sign and magnitude of $V_{II'-II'}$ were constrained by the splitting and intensity of the experimental cross peaks; positive coupling can be ruled out as it leads to the wrong intensity ratio between the high and low frequency features in each structural motif. Previous theoretical work gives evidence in favor of strong through-bond amide II-II coupling, but is of limited comparison because it has not considered deuterated amide groups.^{13,41}

Linear and 2D IR spectra for the AP β sheet, α helix and random coil were calculated for parallel and perpendicular polarizations, and appear in Fig. 4. FTIR spectra

capture the two mode structure of amide II' with different intensity variations for sheets and helices. General trends in the position and amplitude of diagonal and cross peaks, and the interference patterns they participate in are largely reproduced. Experimental and calculated 2D IR spectra are also compared using projections along ω_1 in Fig. 3. For the random coil spectra, lineshapes and intensities of positive and negative contributions are well-reproduced by the calculation, indicating that the two peak structure is not an indicator of a random contour to the chain, but of through-bond coupling that has weak dependence on conformation. The intensity of the low frequency amide II' α helical peak is exaggerated in the calculation and appears as only a shoulder in the experiment. The splitting and intensities of the β sheet projections match the experiment reasonably well. All together these results explain the intensity variation between positive and negative lobes of the peaks without invoking electrical anharmonicity, but rather the result of interference. Agreement between the experiment and calculations demonstrates two points. First, only nearest neighbor coupling is required to reproduce the splitting between amide II' vibrations. Second, the sign and magnitude of this nearest neighbor coupling can be unambiguously obtained from the intensity ratio and splitting observed in the amide I'-II' 2D IR spectra.

Control calculations of FTIR and 2D IR spectra with and without coupling were used to confirm the origin of spectral features (not shown). Amide I'-II' coupling is required for amide I'-II' cross peaks, but not to yield the observed structure in the amide II' lineshape for any of the three structural motifs. Conversely, introducing amide I'-II' coupling without amide II'-II' coupling never causes appreciable splitting in amide II'. Therefore we conclude that amide II' oscillators couple directly to neighboring amide II'

oscillators; a coupling mechanism where amide II' oscillators are indirectly coupled through mutual coupling to the amide I' manifold is insufficient to reproduce any peak structure.

Using the amide II' eigenstates of the LAH, we have visualized the symmetry of the vibrations contributing to the spectral features using doorway mode analysis. This method identifies bright states that carry a majority of the oscillator strength within a restricted frequency region, and color-codes the amplitude and phase of the oscillators involved.^{42,43} These doorway modes are found to have the symmetries expected for the secondary structure. For amide II', two bright states are found that best describe the low and high frequency β -sheet modes: the amide II' sites oscillate in-phase along the β strands (v_{\parallel}) or across the β strands (v_{\perp}), respectively. For the α helix, the bright states also mirror those found for amide I' with A and E_1 symmetry modes with phases aligned parallel and perpendicular to the helix axis, respectively.

The relative angles between transition dipole moments of the doorway modes are calculated for the amide I' and II' modes of the β sheet and α helix and appear in Table 2. In regions where the density of states is too low (< 5 states), a single intense eigenstate was selected. These results correlate very well to the experimentally observed cross peak ratios of parallel and perpendicular 2D IR spectra from Figure 1. As expected the strongest transitions of the amide I' and II' transitions are nearly orthogonal, with a calculated angle of 87° between the transition dipoles. Similarly, the dominant α -helix mode of amide I' runs along the axis while the dominant amide II' is orthogonal. This is observed in both the calculated angles of the amide I A mode relative to the E_1 modes of

amide II' of 72° and 92° and in the experimental polarization spectra. These results are consistent with those presented by Marsh and co-workers.³⁹

Conclusion

We have demonstrated the increased protein secondary structural sensitivity that can be obtained through multi-mode 2D IR spectroscopy. To this point, the amide I vibrational mode of proteins has been predominantly used to provide molecular insight to the protein structure and dynamics. While 2D amide I' spectra improve sensitivity over traditional FTIR, they still cannot readily separate helix and coil absorptions. Amide I'-II' 2D IR experiments on the idealized system of poly-L-lysine in the β -sheet, α -helix, and random coil conformations shows that a combination of amide I' and II' diagonal and cross peaks can more effectively distinguish the secondary structural content. As shown by polarization-selective measurements, this added sensitivity arises from the near-orthogonal transition dipole moments of amide II' relative to amide I', allowing modes of differing symmetry to be correlated.

Modeling of the amide I'-II' FTIR and 2D IR spectra provides insight into the molecular origin of the observed amide II' peaks. We find that negative amide II'-II' couplings between bonded residues and strong on-site amide I'-II' couplings are the two critical features to describe 2D IR spectra. The empirically obtained $V_{II'-II'}$ do not vary significantly with secondary structure: -8.5 cm^{-1} for the β sheet, -8.7 cm^{-1} for the α helix, and -5 cm^{-1} for the coil are found. Through-space amide II' couplings are not required to obtain the basic features of the spectra. These observations suggest that somewhat more sophisticated treatments that allow the site energies and couplings to vary⁴⁴ can be used to obtain amide I'/II' spectra of proteins using MD simulation.^{12,45,46}

The combination of 2D IR spectra and structure-based modeling extends the capabilities of 2D IR spectroscopy to interpret protein conformational changes. Transient 2D IR experiments can be used to directly follow conformational dynamics and kinetics and interpreted with the aid of MD simulation, as demonstrated recently on ubiquitin unfolding using amide I'.⁴⁷ Further, these methods can be used in conjunction with H/D exchange experiments to reveal those secondary structures that are solvent exposed.²¹

Acknowledgements

This work was supported by the National Science Foundation (CHE-0616575), the U.S. Department of Energy (DE-FG02-99ER14988), and the Petroleum Research Fund. R. A. N. thanks the DOD for an NDSEG fellowship.

Supporting Information

Complete amide I'-II' 2D IR spectra of PLL as a function of polarization including expanded diagonal regions. Similar plots are presented for calculated spectra. Also, visualizations of the amide I' and II' modes of protein secondary structures and their transition dipole orientations.

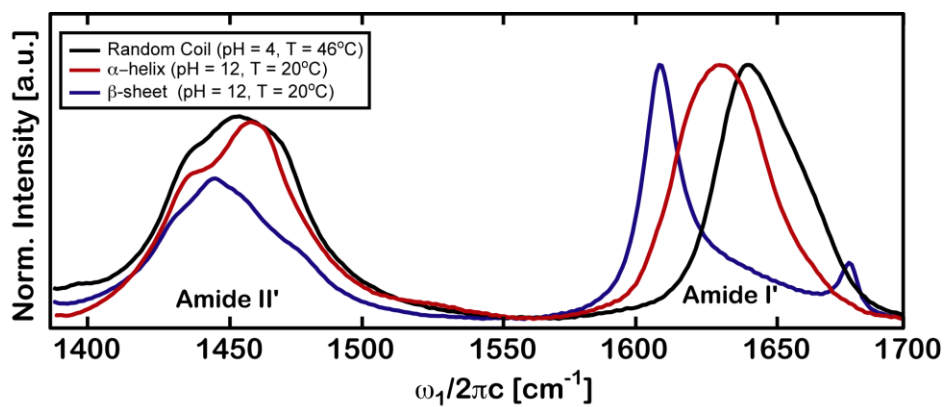


Figure. 1 FTIR spectra of poly-L-lysine as a function of pH and temperature showing the β -sheet (pH=12,T=46°C), α -helix (pH=12,T<20°C) and random coil (pH=4,T=20°C) form of the homopolymer.

2D IR Spectra of Poly-L-Lysine

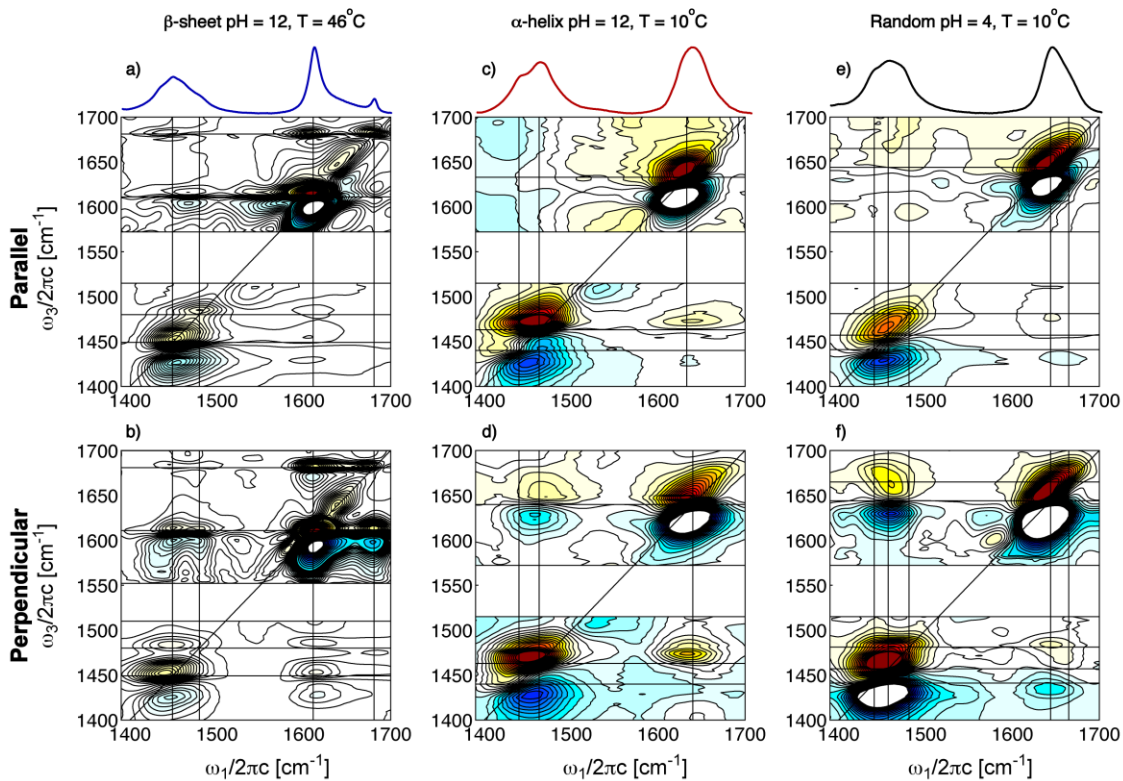


Figure. 2 ZZZZ and ZZZY Amide I'-II' 2D IR spectra of poly-L-lysine as a function of pH and temperature of preparation showing the β -sheet (a,b; pH=12, T=46°C), α -helix (c,d; pH=12, T=20°C) and random coil (e,f; pH=4, T=20°C) forms. Contours are plotted from +/- 80% of the amide I' normalized peak at a 5% spacing. For the β -sheet conformation, contours are plotted at 1.25% between +/- 20% to enhance subtle features of the cross peak region.

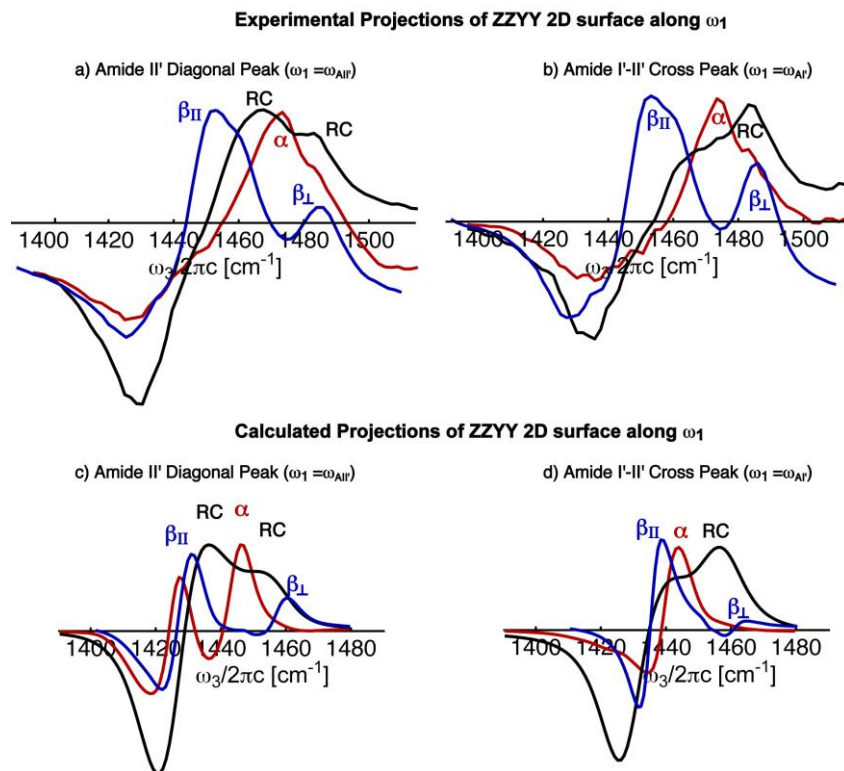


Figure. 3 Comparison of the experimental (a,b) and calculated (c,d) ZZYY 2D IR projections. Projections of the β sheet, α helix and random coil of the amide II' diagonal ($1420-1500 \text{ cm}^{-1}$) and the amide I'-II'' downward cross peak ($1600-1700 \text{ cm}^{-1}$). Projections show identical band structures with inclusion of negative nearest neighbor couplings.

Figure 4 – Calculated 2D IR spectra

Calculated 2D IR Spectra of Idealized Secondary Structure

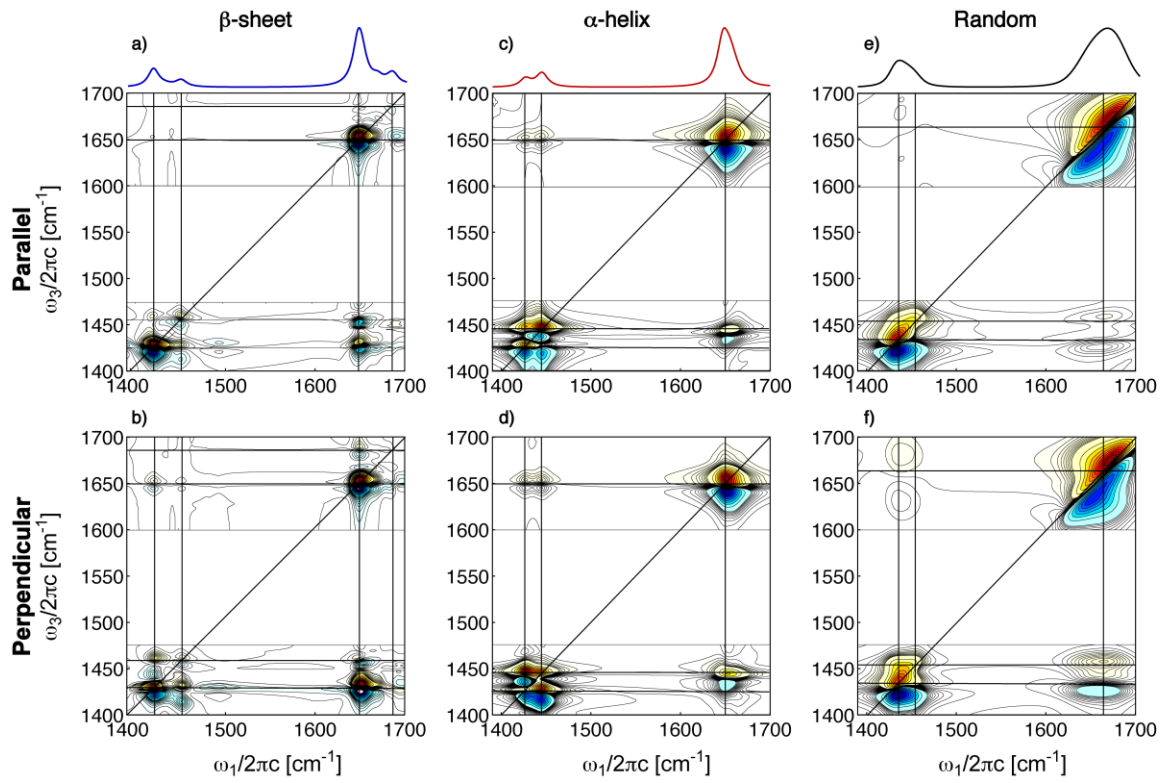


Figure 5: ZZZZ and ZZZY Amide I'-II' 2D IR spectra of concanavalin A, myoglobin, ubiquitin and RNaseA. Contours are plotted from +/- 80% of the amide I' normalized peak at a 4% spacing. In addition for concanavalin A, extra contours are plotted at 1.25% between +/- 20%. The contours of the amide I/II and I'/II' regions are bolded to enhance subtle features of the cross peak regions.

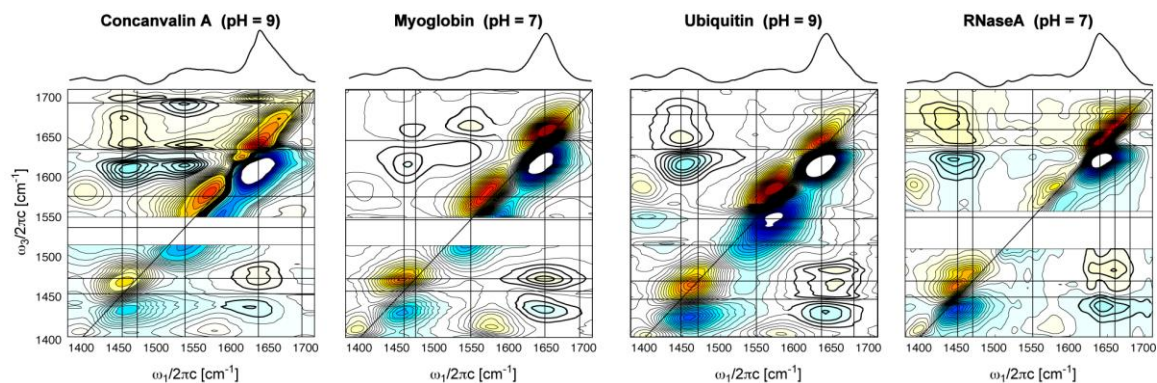


Table 1. Experimentally determined projection angle between amide I' and II' transition dipole moments in poly-L-lysine for sheet, helix, and coil samples. Vibrational frequency assignments to mode symmetry are as discussed in text. $\langle \Theta \rangle$ and constraints on this value are obtained from the ratio of cross peak amplitudes for perpendicular and parallel polarization, using the rules for two coupled vibrations.[ref] Where destructive interference effects limit an accurate determination on angles, the lower bound is given.

β sheet		Amide II'		Amide I'
		ν_{\parallel} 1447 cm^{-1}	ν_{\perp} 1470 cm^{-1}	ν_{\perp} 1611 cm^{-1}
Amide I'	ν_{\parallel} 1690 cm^{-1}	0 \pm 20	60 \pm 8	>67
	ν_{\perp} 1611 cm^{-1}	>70	45 \pm 10	---
Amide II'	ν_{\perp} 1470 cm^{-1}	>35	---	
	ν_p 1447 cm^{-1}	---		

α helix		Amide II'	
		A 1427 cm^{-1}	E_1 1444 cm^{-1}
Amide I'	E_1 1650 cm^{-1}	>60 62 \pm 5?	*
	A 1645 cm^{-1}	*	90 90 \pm 10?

*The dominance of the amide I' A mode and amide II' E_1 modes limits the ability to determine these angles.

Random Coil		Amide II'	
		(-) 1440 cm^{-1}	(+) 1470 cm^{-1}
Amide I'	(+) 1650 cm^{-1}	>60	---
	(-) 1645 cm^{-1}	60	>56
Amide II'	(+) 1470 cm^{-1}	>30	---
		---	---

Table 2. Calculated orientation of the amide I' and II' transition dipole moments for idealized secondary structures. θ defines the angles of the transition dipole relative to the dominant axis of the secondary structure: Along the β -strands for β -sheet and along the α -helix axis. For each mode, the central frequency of the doorway mode or eigenstate is given. Bolded angles represent modes with the strongest cross peaks observed in the perpendicular 2D IR spectra.

		Amide II'					
		θ	ν_p 1425 cm ⁻¹	ν_{perp} 1460 cm ⁻¹	A 1426 cm ⁻¹	E ₁ 1444 cm ⁻¹	E ₁ 1446 cm ⁻¹
Amide I'	θ		91	2	159	92	112
	ν_{\parallel} 1680 cm ⁻¹	61	30	59			
	ν_{perp} 1640 cm ⁻¹	177	87	5			
	A 1645 cm ⁻¹	20			139	72	92
	E ₁ 1650 cm ⁻¹	60			99	32	52
	E ₁ 1657 cm ⁻¹	69			89	23	43

References

- (1) Demirdöven, N.; Cheatum, C. M.; Chung, H. S.; Khalil, M.; Knoester, J.; Tokmakoff, A. *J. Am. Chem. Soc.* **2004**, *126*, 7981-7990.
- (2) Barth, A.; Zscherp, C. *Q. Rev. Biophys.* **2002**, *35*, 369-430.
- (3) Hamm, P.; Lim, M.; Hochstrasser, R. M. *J. Phys. Chem. B* **1998**, *102*, 6123-6138.
- (4) Woutersen, S.; Hamm, P. *J. Phys.: Condens. Mat.* **2002**, *14*, 1035-1062.
- (5) Zanni, M. T.; Hochstrasser, R. M. *Curr. Opin. Struct. Biol.* **2001**, *11*, 516-522.
- (6) Scheurer, C.; Piryatinski, A.; Mukamel, S. *J. Am. Chem. Soc.* **2001**, *123*, 3114.
- (7) DeCamp, M. F.; DeFlores, L. P.; McCracken, J. M.; Tokmakoff, A.; Kwac, K.; Cho, M. *J. Phys. Chem. B* **2005**, *109*, 11016-11026.
- (8) Cheatum, C. M.; Tokmakoff, A.; Knoester, J. *J. Chem. Phys.* **2004**, *120*, 8201-8215.
- (9) Chung, H. S.; Khalil, M.; Tokmakoff, A. *J. Phys. Chem. B* **2004**, *108*, 15332-15343.
- (10) Chung, H. S.; Khalil, M.; Smith, A. W.; Ganim, Z.; Tokmakoff, A. *Proc. Natl. Acad. Sci. USA* **2005**, *102*, 612-617.
- (11) Chung, H. S.; Tokmakoff, A. *J. Phys. Chem. B* **2005**, in press.
- (12) Ganim, Z.; Tokmakoff, A. *Biophys. J.* **2006**, *91*, 2636-2646.
- (13) Hayashi, T.; Mukamel, S. *J. Phys. Chem. B* **2007**, *111*, 11032-11046.
- (14) Jansen, T. I. C.; Knoester, J. *J. Phys. Chem. B* **2006**, *110*, 22910.
- (15) Choi, J.-H.; Lee, H.; Lee, K.-K.; Hahn, S.; Cho, M. *J. Chem. Phys.* **2007**, *126*, 045102.
- (16) Chung, H. S.; Khalil, M.; Smith, A. W.; Tokmakoff, A. *Rev. Sci. Instr.* **2007**, *78*.
- (17) Jackson, M.; Mantsch, H. H. *Crit. Rev. Biochem. Mol.* **1995**, *30*, 95-120.
- (18) Byler, D. M.; Susi, H. *Biopolymers* **1986**, *25*, 469-487.
- (19) Ganim, Z.; Chung, H. S.; Smith, A. W.; DeFlores, L. P.; Jones, K. C.; Tokmakoff, A. *Acc. Chem. Res.* **2008**, *31*, 432-441.
- (20) Krimm, S.; Bandekar, J. *Adv. Protein Chem.* **1986**, *38*, 181-364.
- (21) DeFlores, L. P.; Tokmakoff, A. *J. Am. Chem. Soc.* **2006**, *128*, 16520-16521.
- (22) Miyazawa, T.; Blout, E. R. *J. Am. Chem. Soc.* **1961**, *83*, 712-719.
- (23) Dijkstra, A.; Jansen, T. I. C.; Bloem, R.; Knoester, J. *J. Chem. Phys.* **2007**, *127*, 194505.
- (24) Rosenheck, K.; Doty, P. *Proc. Nat. Acad. Sci.* **1961**, *47*, 1775.
- (25) Davidson, B.; Fasman, G. D. *Biochemistry* **1967**, *6*, 1616-1629.
- (26) DeFlores, L.; Nicodemus, R. A.; Tokmakoff, A. *Opt. Lett.* **2007**, *32*, 2966.

- (27) G.Schaftenaar; Noordik, J. H. *J. Comput.-Aided Mol. Design* **2000**, *14*, 123-134.
- (28) Lindahl, E.; Hess, B.; Spoel, D. v. d. *J. Mol. Mod.* **2001**, *7*, 306-317.
- (29) Berendsen, H. J. C.; Spoel, D. v. d.; Drunen, R. v. *Comp. Phys. Comm.* **1995**, *91*, 43-56.
- (30) Hess, B.; Bekker, H.; Berendsen, H. J. C.; Fraaije, J. G. E. M. *J. Comp. Chem.* **1997**, *18*, 1463-1472.
- (31) Torii, H.; Tasumi, M. *J. Chem. Phys.* **1992**, *96*, 3379-3387.
- (32) DeFlores, L. P.; Ganim, Z.; Ackley, S. F.; Chung, H. S.; Tokmakoff, A. *J. Phys. Chem. B* **2006**, *110*, 18973-18980.
- (33) Golonzka, O.; Tokmakoff, A. *J. Chem. Phys.* **2001**, *115*, 297-309.
- (34) Ganim, Z.; Chung, H. S.; Smith, A.; DeFlores, L.; Jones, K. C.; Tokmakoff, A. *Acc. Chem. Res.* **2008**.
- (35) Khalil, M.; Demirdoven, N.; Tokmakoff, A. *J. Phys. Chem. A* **2003**, *107*, 5258-5279.
- (36) Woutersen, S.; Hamm, P. *J. Chem. Phys.* **2001**, *115*, 7737-7743.
- (37) Fang, C.; Wang, J.; Charnley, A. K.; Barber-Armstrong, W.; Smith, A. B.; Decatur, S. M.; Hochstrasser, R. M. *Chem. Phys. Lett.* **2003**, *382*, 586-592.
- (38) Ham, S.; Hahn, S.; Lee, C.; Kim, T.-K.; Kwak, K.; Cho, M. *J. Phys. Chem. B* **2004**, *108*, 9333-9345.
- (39) Marsh, D.; Muller, M.; Schmitt, F. *Biophys J.* **2000**, *78*, 2499-2510.
- (40) Fändrich, M.; Dobson, C. M. *EMBO J.* **2002**, *21*, 5682-5690.
- (41) Moran, A.; Mukamel, S. *Proc. Natl. Acad. Sci. USA* **2004**, *101*, 506-510.
- (42) Chung, H. S.; Tokmakoff, A. *Journal of Physical Chemistry B* **2006**, *110*, 2888-2898.
- (43) Torii, H.; Tasumi, M. *J. Chem. Phys.* **1992**, *97*, 92-98.
- (44) Bloem, R.; Dijkstra, A. D.; Jansen, T. I. C.; Knoester, J. *J. Chem. Phys.* **2008**, *129*, 055101
- (45) Ham, S.; Cho, M. *J. Chem. Phys.* **2003**, *118*, 6915-6922.
- (46) Jansen, T. I. C.; Knoester, J. *J. Chem. Phys.* **2006**, in press.
- (47) Chung, H. S.; Ganim, Z.; Jones, K. C.; Tokmakoff, A. *Proc. Nat. Acad. Sci.* **2007**, *104*, 14237-14242.